

Crystalline Silicon Solar Cells with Two Different Metals

Toshiyuki Sameshima*, Kazuya Kogure, and Masahiko Hasumi

Tokyo University of Agriculture and Technology, 2-24-16 Naka-cho, Koganei, Tokyo 184-8588, Japan

Received June 21, 2010; accepted July 25, 2010; published online November 5, 2010

We propose crystalline silicon solar cells with Al and Au metals. P-type substrates were coated with 100-nm-thick thermally grown SiO₂ layers. The top SiO₂ layer was thinned to about 1.5 nm. Stripes of Al and Au were formed with a gap of 0.29 mm on the top surface in order to cause an internal built-in potential in silicon because of the difference between their work functions. Solar cell characteristics were observed by halogen lamp illumination at 21.7 mW/cm². The short-circuit current density, open-circuit voltage, and fill factor were 5.8 mA/cm², 0.49 V, and 0.57. The conversion efficiency was 7.5%. Photo-induced holes and electrons flowed into Au and Al electrodes, respectively, by the tunneling effect.

© 2010 The Japan Society of Applied Physics

DOI: 10.1143/JJAP.49.110205

Semiconductor solar cells have been attractive as a device for producing electrical power from sunlight.¹⁾ The conversion power efficiency and production cost are essential points in the advancement of the solar cell industry and its business. Many important technologies have been developed to improve those points, such as shallow PN junction formation, back-surface field formation, defect passivation, and multijunction formation.^{2,3)} Simple processing is still attractive for the low-cost fabrication of solar cells.

In this paper, we propose a simple semiconductor solar cell with two different kinds of metals. No PN junction formation is necessary. We first discuss the physics of our solar cell model. We then experimentally demonstrate the fabrication of a solar cell based on our model. We report the characteristics of our solar cell and discuss its technical possibilities.

Figure 1(a) shows a schematic image of the energy band structure of our solar cell model. Two different metals, aluminum (Al) and gold (Au), are selected. Their work functions are reported as 4.18 and 5.1 eV, respectively.⁴⁾ When p-type crystalline silicon is sandwiched by Al and Au metals, the difference in the work functions of those metals can cause an internal built-in potential in the silicon. Because the initial Fermi level of silicon is near the work function of Au but far different from that of Al, a large internal potential distribution associated with the depletion region is spatially formed near the Al metal electrode, as shown in Fig. 1(a). Holes and electrons excited by light illumination in silicon separate from each other according to the internal potential distribution. Holes move toward the Au electrode, and electrons move toward the Al electrodes. However, it is well known that a high density of surface states limits the internal potential height to be low and causes serious recombination of holes and electrons. The semiconductor surface should be passivated to generate a high built-in potential. We therefore introduce thin SiO₂ layers between the silicon and the two metals, as shown in Fig. 1(a), because the SiO₂/Si interface is stable and has a low density of interface states. SiO₂ will maintain a high internal built-in potential barrier. An SiO₂ layer thinner than 2 nm is essential to achieve photo-induced carrier flow from silicon to the two metals by the tunneling effect.⁵⁾ The conventional metal-insulator-semiconductor (MIS) solar cell or Schottky-barrier solar cell⁶⁻¹²⁾ also has a depletion

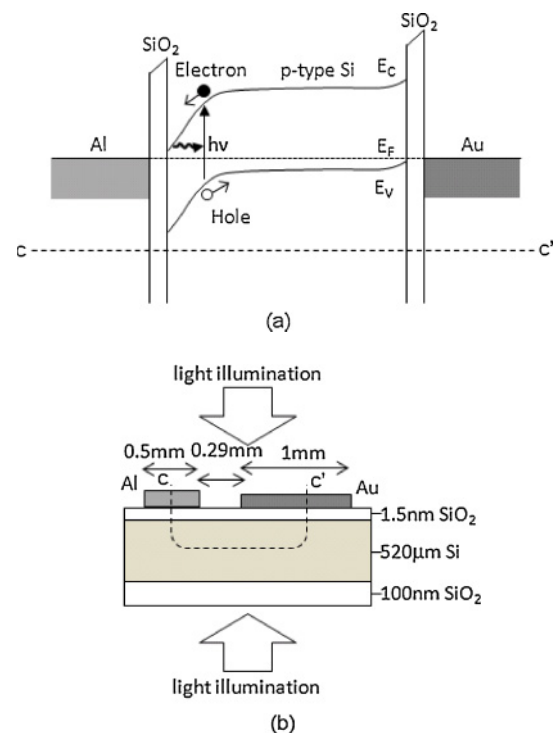


Fig. 1. (Color online) Schematic energy band image of present solar cell (a) and schematic cross section of experimental solar cell structure and light illumination image for measurement of solar cell characteristics (b). The band structure is along dashed curve *c-c'*.

layer formed near one metal electrode, caused by the difference in the work functions between the metal and silicon. However, the other metal electrode is in direct contact with the silicon substrate in those solar cells. In most cases, the surface of silicon is doped to achieve an ohmic contact with the metal. In contrast, the silicon in our solar cell shown in Fig. 1(a) is not in direct contact with any metal electrode and its surfaces are passivated with thin insulator layers. No doping or PN junction formation in silicon is necessary because the difference in the work functions of the metals causes an internal built-in potential in a semiconductor. The tunneling effect allows current to pass through the thin insulators.

Figure 1(b) shows a schematic cross section of the solar cell fabricated with Al and Au metals and a light illumination image for the measurement of solar cell characteristics. P-type single-crystalline silicon substrates with a thickness of 520 μm and a resistivity of 30 Ω cm were

*E-mail address: tsamesim@cc.tuat.ac.jp

used. The band structure shown in Fig. 1(a) is along the dashed curve in Fig. 1(b). The top mirror-polished surface and rough rear surface were thermally oxidized, and 100-nm-thick thermally grown SiO₂ layers were formed on both surfaces. The SiO₂ layer at the top surface was then thinned with buffered hydrofluoric acid. Thin SiO₂ slightly decreased the optical reflectivity of the surface because of antireflective interference effect. The thickness of SiO₂ was estimated to be about 1.5 nm by analyzing the optical reflectivity spectra.¹³⁾ Samples were then annealed at 260 °C for 3 h in 1.3 × 10⁶ Pa H₂O vapor to passivate the silicon surface.¹⁴⁾ On the top surface, stripes of Al with a width of 0.5 mm and Au with a width of 1.0 mm were formed with a gap of 0.29 mm by thermal evaporation. Electrical current as a function of voltage was measured under halogen lamp light illumination at 21.7 mW/cm² to the top and rear surfaces. Samples with only Al stripes were also fabricated for comparison.

The minority carrier effective lifetime, τ_{eff} , was measured by 9.35 GHz microwave transmission measurement.¹⁵⁾ τ_{eff} was 185 μs for the initial silicon substrates with both surfaces coated with 100-nm-thick SiO₂ layers. The silicon surface was well passivated by the SiO₂ layers. When the thickness of SiO₂ films at the top surface was decreased to about 1.5 nm using buffered hydrofluoric acid, τ_{eff} decreased to 16 μs . This means that the carrier recombination rate at the top surface was increased after SiO₂ etching. The subsequent 1.3 × 10⁶ Pa H₂O vapor heat treatment at 260 °C for 3 h increased τ_{eff} to 47 μs . Surface passivation was improved by the high-pressure H₂O heat treatment and τ_{eff} increased. However, τ_{eff} did not return to the initial value under the above conditions. Figure 2 shows the absolute electrical current as a function of voltage for samples with Al and Au stripes (a) and samples with only Al stripes (b), in the dark and illuminated with light to the rear surfaces. The electrical current increased as the voltage increased under the dark condition. We believe that tunneling current was observed. Light illumination markedly increased the electrical current. A substantial current at 0 V, indicating the short-circuit current density, was observed for the sample with Al and Au stripes, as shown in Fig. 2(a). It indicates that photo-induced current was generated because holes and electrons were separated and flowed toward Au and Al, respectively, in accordance with the internal built-in potential. No current appeared at 0.49 V, indicating an open-circuit voltage. On the other hand, no current appeared at 0.02 V for the sample with only Al stripes, as shown in Fig. 2(b). There was no substantial power generation for samples with only Al stripes because almost the same internal potential distribution was formed underneath Al stripes. Figure 3 shows solar cell characteristics with light illumination to the rear and top surfaces for samples with Al and Au stripes with the structure shown in Fig. 1(b). Typical solar cell current voltage characteristics were obtained. In the case of light illumination to the rear surface, the short-circuit current density J_{sc} , the open-circuit voltage V_{oc} , and fill factor FF were 5.8 mA/cm², 0.49 V, and 0.57, respectively. The conversion efficiency was therefore 7.5%. Holes and electrons generated at the rear surface traveled across the 520- μm -thick silicon substrate and flowed into Au and Al, respectively. In the case of light illumination to the top

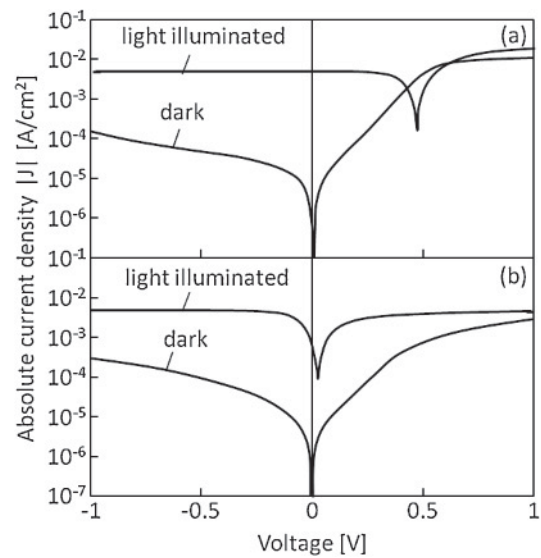


Fig. 2. Absolute electrical current as a function of voltage for samples with Al and Au stripes (a) and samples with only Al stripes (b) in the dark and with light illuminated to the rear surfaces.

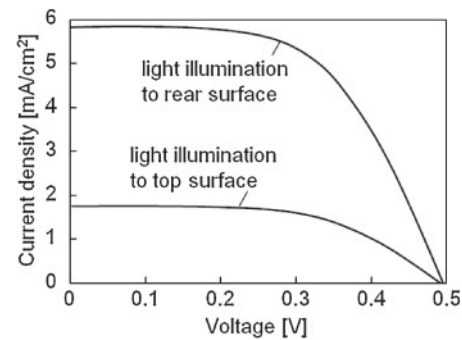


Fig. 3. Solar cell characteristics for light illumination to the rear and top surfaces for samples with Al and Au stripes.

surface, V_{oc} and FF were 0.48 V and 0.57, respectively. On the other hand, J_{sc} was 1.8 mA/cm² lower than that for illumination to the rear surface because the top surface was shaded by Al and Au electrodes.

The results in Figs. 2 and 3 demonstrate our solar cell model discussed above. However, the present fabrication process was not yet optimized. The series resistivity was estimated to be about 20 Ωcm^2 from the minimum differential resistivity of the solar cell characteristic for illumination to the rear surface shown in Fig. 3. The V_{oc} of 0.49 V suggests that the two thin SiO₂ layers in the solar cell in Fig. 1(b) were effectively biased by 0.43 V because the difference in the work functions of Al and Au was 0.92 eV. We roughly estimate that each SiO₂ layer was biased by 0.22 V and had an effective resistivity of 10 Ωcm^2 . According to Lo *et al.*'s report,⁵⁾ SiO₂ layers had effective resistivities of 4 × 10⁻³, 2, and 2 × 10³ Ωcm^2 with thicknesses of 1, 1.5, and 2 nm, respectively, when they were applied with 0.2 V. This simple estimation indicates that the SiO₂ thickness was probably greater than 1.5 nm. Moreover, the SiO₂ thickness was not uniform over the substrate. The solar cell characteristics therefore vary locally at the present stage. A formation process of thin SiO₂ should be estab-

lished in order to reduce the serial resistance accompanied with increasing FF . τ_{eff} of $47\ \mu\text{s}$ was short because the effective carrier diffusion length $(D\tau_{\text{eff}})^{0.5}$ was low, about $410\ \mu\text{m}$, where D is the diffusion coefficient of electrons. A surface passivation process should be established to achieve a long τ_{eff} under the condition of SiO_2 with a thickness of around $1.5\ \text{nm}$. The width of metal stripes and their gap width should be much lower than the effective carrier diffusion length to effectively collect photo-induced carriers. Fine metal electrodes and their patterning must be investigated. A thin substrate should be used for effective carrier diffusion when light is illuminated to the rear surface. We believe that no doping results in a high-efficiency solar cell comparable to conventional silicon solar cells via the optimization of the fabrication processes as discussed above, because there is no carrier recombination associated with defects induced by impurity doping. For our solar cell model, it is essential that the difference in the work functions of two different kinds of metals causes an internal built-in potential in the semiconductor. Many other choices of metals will be possible besides the Al–Au pair used in the present work. For example, a combination of Hf and Au has a large difference of $1.2\ \text{eV}$ in the work function.⁴⁾ This has the advantage of causing a high internal built-in potential in silicon. Many semiconductors may be used if their work functions are between those of the two different metals.

In summary, crystalline silicon solar cells were demonstrated. P-type $520\text{-}\mu\text{m}$ -thick $30\ \Omega\ \text{cm}$ single-crystalline silicon substrates coated with 100-nm -thick thermally grown SiO_2 layers were used. The SiO_2 layer at the top surface was thinned to about $1.5\ \text{nm}$ using buffered hydrofluoric acid. Samples were then annealed at $260\ ^\circ\text{C}$ for $3\ \text{h}$ in $1.3 \times 10^6\ \text{Pa}$ H_2O vapor. The minority carrier effective lifetime was $47\ \mu\text{s}$. Stripes of Al with a width of $0.5\ \text{mm}$ and Au with a width of $1.0\ \text{mm}$ were formed with a gap of $0.29\ \text{mm}$ on the top surface by thermal evaporation. Electrical current as a

function of voltage was measured between Al and Au stripes under light illumination of a halogen lamp at $21.7\ \text{mW}/\text{cm}^2$ to the rear surface. Typical current voltage characteristics of solar cells were obtained. J_{sc} , V_{oc} , and FF were $5.8\ \text{mA}/\text{cm}^2$, $0.49\ \text{V}$, and 0.57 , respectively. The conversion efficiency was 7.5% . Holes and electrons generated at the rear surface traveled across the $520\text{-}\mu\text{m}$ -thick silicon substrate and flowed into Au and Al electrodes, respectively, owing to a tunneling effect. These results demonstrated our solar cell physics that a difference in the work functions of two different kinds of metals causes an internal built-in potential in silicon.

Acknowledgment This work was partly supported by a Grant-in-Aid for Science Research C (No. 22560292) from the Ministry of Education, Culture, Sports, Science and Technology, Japan.

- 1) A. Rohatagi: Proc. 3rd World Conf. Photovoltaic Energy Conversion, 2003, p. A29.
- 2) M. A. Green: *Prog. Photovoltaics* **17** (2009) 183.
- 3) K. Yamamoto: *Sol. Energy Mater. Sol. Cells* **66** (2001) 117.
- 4) H. B. Michaelson: *J. Appl. Phys.* **48** (1977) 4729.
- 5) S.-H. Lo, D. A. Buchanan, Y. Tauer, and W. Wang: *IEEE Electron Device Lett.* **18** (1997) 209.
- 6) M. A. Green and R. B. Godfrey: *Appl. Phys. Lett.* **29** (1976) 610.
- 7) R. B. Godfrey and M. A. Green: *Appl. Phys. Lett.* **34** (1979) 790.
- 8) P. K. Dubey and V. V. Paranjape: *J. Appl. Phys.* **48** (1977) 324.
- 9) J. Shewchun, R. Singh, and M. A. Green: *J. Appl. Phys.* **48** (1977) 765.
- 10) C.-J. Huang, M.-P. Houng, Y.-H. Wang, N.-F. Wang, and W.-J. Chang: *Jpn. J. Appl. Phys.* **37** (1998) L158.
- 11) Y.-P. Shen and J.-G. Hwu: *IEEE Photonics Technol. Lett.* **8** (1996) 420.
- 12) F. Horikiri, T. Ichikawa, L. Q. Han, A. Kaimai, K. Yashiro, H. Matsumoto, T. Kawada, and J. Mizusaki: *Jpn. J. Appl. Phys.* **44** (2005) 8023.
- 13) T. Sameshima, N. Andoh, and Y. Andoh: *Jpn. J. Appl. Phys.* **44** (2005) 1186.
- 14) T. Sameshima and M. Satoh: *Jpn. J. Appl. Phys.* **36** (1997) L687.
- 15) T. Sameshima, H. Hayasaka, and T. Haba: *Jpn. J. Appl. Phys.* **48** (2009) 021204.